BIOCHEMISTRY
including biophysical chemistry & molecular biology
Article

Biochemistry **2011,** *50,* 419–425 419
DOI: 10.1021/bi1010893

Pre-Steady-State Kinetic Analysis of Enzyme-Monitored Turnover during Cystathionine β-Synthase-Catalyzed H_2S Generation[†]

Sangita Singh, David P. Ballou, and Ruma Banerjee*

Department of Biological Chemistry, University of Michigan Medical Center, Ann Arbor, Michigan 48109-0600, United States

Received July 7, 2010; Revised Manuscript Received December 9, 2010

ABSTRACT: Cystathionine β-synthase (CBS) catalyzes the first step in the transsulfuration pathway in mammals, i.e., the condensation of serine and homocysteine to produce cystathionine and water. Recently, we have reported a steady-state kinetic analysis of the three hydrogen sulfide (H_2S)-generating reactions that are catalyzed by human and yeast CBS [Singh, S., et al. (2009) *J. Biol. Chem. 284*, 22457−22466]. In the study presented here, we report a pre-steady-state kinetic analysis of intermediates in the H_2S-generating reactions catalyzed by yeast CBS (yCBS). Because yCBS does not have a heme cofactor, in contrast to human CBS, it is easier to observe reaction intermediates with yCBS. The most efficient route for H_2S generation by yCBS is the β-replacement of the cysteine thiol with homocysteine. In this reaction, yCBS first reacts with cysteine to release H_2S and forms an aminoacrylate intermediate (k_{obs} of 1.61 ± 0.04 mM^{-1} s^{-1} at low cysteine concentrations and 2.8 ± 0.1 mM^{-1} s^{-1} at high cysteine concentrations, at 20 °C), which has an absorption maximum at 465 nm. Homocysteine binds to the E·aminoacrylate intermediate with a bimolecular rate constant of 142 mM^{-1} s^{-1} and rapidly condenses to form the enzyme-bound external aldimine of cystathionine. The reactions could be partially rate limited by release of the products, cystathionine and H_2S.

Hydrogen sulfide (H_2S),[1] like nitric oxide and carbon monoxide, is a gaseous signaling molecule (*1*−*3*) that elicits a variety of physiological effects. In the cardiovascular system, H_2S apparently functions as a vasorelaxant (*4*) and as a cardioprotective agent (*5*). A dose-dependent decrease in murine blood pressure by sodium hydrosulfide has been reported (*4*). Other reported effects of H_2S include protection against ischemia reperfusion injury and anti-inflammatory effects in tissues (*5*, *6*). In lower organisms like yeast, H_2S plays a role in population synchronization during ultradian oscillations (*7*). There are two known mammalian enzymes that can directly generate H_2S: cystathionase γ-lyase (CGL) and CBS (*8*). A third enzyme pair, 3-mercaptopyruvate sulfurtransferase together with cysteine aminotransferase, catalyzes the transfer of sulfur to an unknown acceptor and, in the presence of a reductant, can liberate H_2S (*3*, *9*). The role of CGL-dependent H_2S production in the vasculature is controversial, with one group reporting development of age-related hypertension in CGL knockout mice (*4*) and another, a normotensive phenotype (*10*).

We have recently demonstrated that human CGL catalyzes H_2S production via five alternative reactions that involve chemistry at either the β carbon or the γ carbon of the substrates, cysteine and homocysteine (*11*). In contrast, CBS generates H_2S via chemistry at the β carbon of the substrate, cysteine (*12*). The contribution of the mercaptopyruvate sulfurtransferase system to H_2S biogenesis relative to the transsulfuration pathway is not known.

CBS catalyzes the condensation of serine and homocysteine to produce cystathionine in the transsulfuration pathway (Scheme 1, reaction 1) (*13*). This reaction provides an avenue for clearing homocysteine in mammals (*14*, *15*). CBS deficiency leads to accumulation of homocysteine and is accompanied by clinical impairments in four major organ systems: the ocular, cardiovascular, central nervous, and skeletal systems (*16*). CBS also catalyzes the condensation of cysteine and homocysteine (reaction 2) or of two molecules of cysteine (reaction 3) to produce cystathionine or lanthionine, respectively (*12*). In both these cysteine-dependent reactions, H_2S is released as a byproduct. Alternatively, CBS can catalyze the β-elimination of H_2S from cysteine and the rehydration of the resulting aminoacrylate to form serine (reaction 4). The k_{cat} for the generation of H_2S by yCBS (55 s^{-1} at 37 °C) via the condensation of cysteine and homocysteine (reaction 2) is 18-fold faster than that for the β-elimination and rehydration to form serine (3 s^{-1}). The condensation of 2 mol of cysteine to form lanthionine occurs at an intermediate rate (8 s^{-1}); however, the K_M for the second mole of cysteine is much larger (33 mM) than that for homocysteine (0.13 mM), so that formation of lanthionine is not expected to compete well with formation of cystathionine at physiological concentrations of substrates. The catalytic turnover numbers for cystathionine formation via reaction 2 by hCBS and yCBS are comparable (55 and 20 s^{-1}, respectively), but the β-elimination of H_2S from cysteine and the subsequent addition of H_2O to form serine with hCBS occurs at a rate of only 0.4 s^{-1} (i.e., 50-fold slower than for formation of cystathionine). As with yCBS, the K_M for the second mole of cysteine (27 mM) is also high for hCBS compared to the affinity of that site for homocysteine (3 mM).

[†]This work was supported in part by grants from the National Institutes of Health (HL58984 to R.B. and GM20877 to D.P.B.).

*To whom correspondence should be addressed: 3320B MSRB III, 1150 W. Medical Center Dr., University of Michigan, Ann Arbor, MI 48109-0600. Telephone: (734) 615-5238. Fax: (734) 763-4581. E-mail: rbanerje@umich.edu.

[1]Abbreviations: CBS, cystathionine β-synthase; yCBS, yeast cystathionine β-synthase; hCBS, human cystathionine β-synthase; PLP, pyridoxal phosphate; H_2S, hydrogen sulfide; CGL, cystathionine γ-lyase.

Published on Web 12/09/2010

Scheme 1

$$\text{Serine} + \text{Homocysteine} \rightarrow \text{Cystathionine} + H_2O \quad [1]$$

$$\text{Cysteine} + \text{Homocysteine} \rightarrow \text{Cystathionine} + H_2S \quad [2]$$

$$\text{Cysteine} + \text{Cysteine} \rightarrow \text{Lanthionine} + H_2S \quad [3]$$

$$\text{Cysteine} + H_2O \rightarrow \text{Serine} + H_2S \quad [4]$$

CBS belongs to the fold II family of PLP enzymes (*17*). Other members of this family include *O*-acetylserine sulfhydrylase, threonine deaminase, and tryptophan synthase (*18*). The presence of PLP and the absence of other chromophores in these enzymes have facilitated extensive kinetic analyses of their reaction intermediates (*19*, *20*). However, the UV−visible absorption spectrum of hCBS is dominated by the strongly absorbing heme chromophore, which compromises direct observation of PLP-bound intermediates during the catalytic cycle (*21*); thus, only limited kinetic analysis of an unstable variant lacking the N-terminal heme domain has been reported (*22*). Hence, the homologous yCBS, which lacks the heme but catalyzes the same PLP-dependent chemical reactions, has been used as a model of the human enzyme to elucidate the kinetic mechanism of the canonical β-replacement reaction (Scheme 1, reaction 1) (*23*, *24*).

In this study, we have analyzed the reaction intermediates formed during biogenesis of H_2S by yCBS via the β-replacement of the cysteine thiol with homocysteine (reaction 2) or by the β-elimination of the cysteine thiol (reaction 3). Our results demonstrate that the kinetics for the H_2S-generating reactions differ from those for the canonical reaction 1, primarily in the first step, i.e., binding of serine or cysteine. Once the common aminoacrylate intermediate is formed from either substrate, the kinetics of the subsequent addition reactions with homocysteine are similar. Under multiple-turnover conditions, the reactions appear to be partially limited by product release.

EXPERIMENTAL PROCEDURES

Materials. L-Cysteine, DL-homocysteine, L-cystathionine, L-serine, and PLP were purchased from Sigma. Protease tablets were purchased from Roche.

Purification of yCBS. The purification of full-length yCBS was adapted from the work of Jhee et al. (*25*) with a slight modification. The pSEC plasmid encoding yCBS was provided by Dr. Edith Miles (National Institutes of Health). *Escherichia coli* strain BL21(DE3) was freshly transformed with the pSEC plasmid. Cells (18 g) obtained from a 1 L culture were suspended in 50 mL of 10 mM potassium phosphate (KP_i) buffer (pH 7.8) containing 1 protease tablet, 100 μM PLP, 10 mM β-mercaptoethanol, 1 mM EDTA, 20 mg of lysozyme, and Triton (0.1%, v/v). Cells were disrupted by sonication using a power output of 7 for nine cycles of 30 s pulses and 3 min breaks. The supernatant obtained after centrifugation at 12000*g* was loaded onto a 16 cm × 4 cm Q-Sepharose column pre-equilibrated with buffer A [10 mM KP_i (pH 7.8)] and washed with buffer A containing 10 mM NaCl. The fractions were eluted with an 800 mL gradient from 0.01 to 0.5 M NaCl in buffer A, and CBS-containing fractions were pooled, concentrated, and dialyzed overnight against buffer A. The protein was then loaded onto a 16 cm × 4 cm hydroxylapatite column pre-equilibrated with buffer A and washed with the same buffer. Protein was eluted with a 600 mL gradient from 0.01 to 0.5 M KP_i (pH 7.8). Fractions of interest were pooled, concentrated, dialyzed against 100 mM HEPES (pH 7.4), and stored at −80 °C. From 1 L of culture, ~300 mg of protein was obtained and was judged to be >95% pure by sodium dodecyl sulfate−polyacrylamide gel electrophoresis analysis. All the purification steps were performed at 4 °C.

Scheme 2

$$E + S \underset{k_2}{\overset{k_1}{\rightleftharpoons}} E.S \underset{k_4}{\overset{k_3}{\rightleftharpoons}} E{\cdot}AA$$

CBS Activity Assays. CBS activity was measured either in the radiolabeled assay (for generation of cystathionine) or in a spectrophotometric assay (for generation of H_2S) as described previously (*12*).

Rapid-Scanning Stopped-Flow Spectroscopy. Pre-steady-state experiments were performed using an Applied Photophysics (Leatherhead, U.K.) stopped-flow spectrophotometer (SX. MV18) in the photodiode-array mode or with a Hi-Tech Scientific (Bradford on Avon, U.K.) stopped-flow spectrophotometer (model SF-61DX) in both single-wavelength and diode-array modes. For diode-array assays, a 1.5 ms integration time was used. The temperature was maintained at 20 °C using a circulating water bath. Double-mixing experiments were conducted using the Hi-Tech stopped-flow spectrophotometer. All concentrations of reagents listed for the stopped-flow experiments are those prior to mixing. In single-mixing experiments, yCBS (70−145 μM, calculated per 55 kDa monomer) was mixed with various concentrations of substrate in 100 mM HEPES (pH 7.4). For L-cystathionine, the stock solution was made in 100 mM HEPES (pH 7.4), followed by the gradual addition of 5 M NaOH until the solution was clear. Further dilutions of cystathionine were made in 100 mM HEPES (pH 7.4). The substrate and enzyme solutions were filtered through a 0.45 μm filter just prior to their use in the stopped-flow experiment.

In the double-mixing experiments, 120 μM yCBS was initially mixed with 30 mM L-serine or L-cysteine in the first step, and after ~15 ms, it was mixed with an equal volume of buffer. The reaction was monitored at 465 nm to determine when the formation of the aminoacrylate intermediate was maximal. On the basis of this information, the delay time was set at 300 ms (with serine) or 500 ms (with cysteine) prior to the second mixing step. After the solution had been aged for the specified time, the aminoacrylate intermediate was rapidly mixed with various concentrations of DL-homocysteine (0.4−40 mM).

Data from the stopped-flow experiments were fitted using the pro-viewer Software (Applied Photophysics), KinetAsyst (Hi-Tech), Specfit Global Analysis Program (Spectrum Software Associates), or Sigma plot. First-order rate constants (k_{obs}) for the reactions with serine, cysteine, and cystathionine were determined from fits to single-exponential or multiple-exponential equations. The k_{obs} values obtained at various concentrations of substrates were fitted to a linear equation to obtain the apparent second-order rate constants.

The observed rate constants, k_{obs}, for the reaction of serine and cystathionine with yCBS (described in Scheme 2) to form an aminoacrylate intermediate show a hyperbolic dependence on substrate concentration, and the data were fitted using eq 1.

$$k_{obsd} = \frac{k_3\,[substrate]}{K_{21} + [substrate]} + k_4 \quad (1)$$

where $K_{21} = k_2/k_1$ and substrate denotes either serine or cystathionine.

RESULTS

Reaction of yCBS with Serine or Cysteine. The UV−visible spectrum of yCBS as isolated exhibits an absorption maximum at 409 nm, which corresponds to the protonated Schiff base (internal aldimine) between Lys53 in the active site and the PLP as described previously (*25*). Addition of serine results in formation of a PLP adduct of the aminoacrylate species with an absorption maximum at 465 nm and apparent isosbestic points with the initial spectrum of the internal aldimine at 425 and 357 nm (Figure 1). However, careful inspection of the kinetic traces near 425 nm reveals two kinetic phases suggesting formation of transient species. The dependencies of the rates of formation of the transient and the aminoacrylate species are shown in Figure 1B. We note that conversion of the internal aldimine to the external aldimine occurs in multiple steps and intermediates are not well resolved either kinetically or spectroscopically in our experiments. Nevertheless, the rate of formation of the aminoacrylate showed a hyperbolic dependence on serine concentration (Figure 1B). Using eq 1, the maximum rate for aminoacrylate formation and the K_{dapp} for serine were estimated to be 155 ± 7 s^{-1} and 14.4 ± 1.7 mM, respectively. At wavelengths near 425 nm, two phases could be detected. The linear dependence of the first phase (k_{obs}) for formation of the apparent transient species on serine is plotted in Figure 1B, but its interpretation is complex. Hence, the apparent bimolecular rate constant (37.8 ± 3.0 mM^{-1} s^{-1}) does not simply correspond to the k_1 (i.e., the binding of serine to enzyme). Because there are several kinetically unresolved steps involved in the formation of the aminoacrylate from serine, we cannot unambiguously assign the observed kinetic phases to specific rate constants, i.e., formation of the external aldimine, or obtain a true K_d for serine. If this were a true second-order reaction to form bound serine, the plot would have an intercept corresponding to k_{-1} and the k_{-1}/k_1 ratio would give the apparent K_d. However, the intercept is near zero such that the measured ratio would be far less than the apparent K_d. Likewise, the maximum extrapolated rate is not k_2. The maximum rate is limited by the maximum equilibrium concentration of the species (presumably the external aldimine) converting to the aminoacrylate.

Global fitting analysis of the spectral data, using the A → B → C model, was used as a first-order approximation for the process and yielded the spectra shown in Figure 1C. We assign spectra a and c primarily to the internal aldimine and the aminoacrylate, respectively. Spectrum b represents the mixture of species that we term the complex transient species. However, spectrum b is similar to that previously assigned to the external aldimine for yCBS at pH 8.0 in Tris buffer (*23*), conditions that better resolved the processes. However, unlike the spectrum obtained for the external aldimine at pH 8.0 (*23*), the corresponding deconvoluted spectrum b in this study is not pure and even shows a small contribution of the 465 nm aminoacrylate species. As noted above, conversion of the internal aldimine (primarily spectrum a) to the external aldimine occurs in multiple steps, and the intermediate gem-diamine species that is formed during the reaction is not detected. Hence, the determined rate constant in fact is complex and comprises multiple component steps that cannot be deconvoluted in this study. The spectral changes resulting from the addition of cysteine to yCBS are shown in Figure 2A. Upon addition of cysteine, the absorption maximum

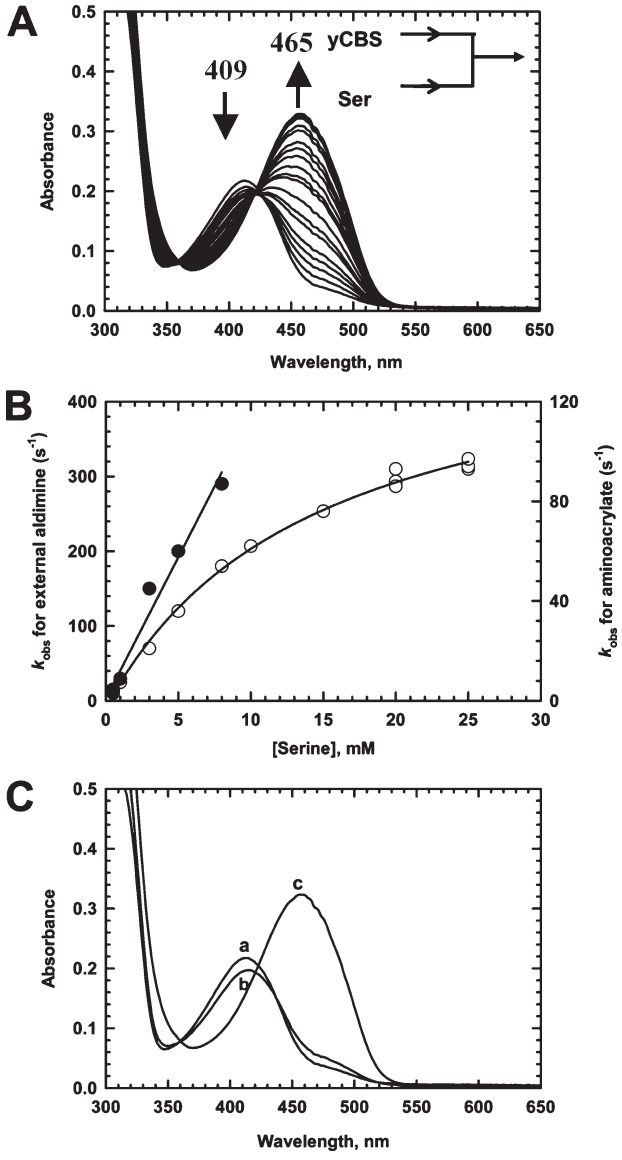

FIGURE 1: Spectra obtained by rapid-scanning stopped-flow spectrophotometry of the reaction of yCBS with serine in 100 mM HEPES buffer (pH 7.4) at 20 °C. (A) yCBS (55 μM) was mixed with 16 mM L-serine, and spectra were recorded for 1.4 s. The internal aldimine has an absorption maximum at 409 nm, and upon addition of serine, it converts to the aminoacrylate intermediate with an absorption maximum at 465 nm. (B) Dependence of the observed first-order rate constants for the formation of aminoacrylate at 465 nm (○, right axis) and appearance of the transient species observed at ~425 nm (●, left axis) on the concentration of L-serine. (C) Deconvolution of the rapid scan data shown in panel A. Spectra a−c are assigned to the internal aldimine, the transient species with characteristics consistent with it having external aldimine spectral character, and the aminoacrylate, respectively. The initially observed spectrum at ~1.5−2 ms already has a small contribution of the aminoacrylate species, which would be expected in the rapid reactions involving 16 mM serine. At this concentration, panel B shows that the rate of formation of the aminoacrylate is ~250 s^{-1}.

shifts from 409 to 465 nm, very similar to the change seen with the addition of serine. The rate of disappearance of the internal aldimine or formation of the aminoacrylate intermediate was not linearly dependent on cysteine concentration (Figure 2B). At cysteine concentrations of < 15 mM, a bimolecular rate constant of 1.61 ± 0.04 mM^{-1} s^{-1} was estimated, and at cysteine concentrations of > 20 mM, a bimolecular rate constant of 2.8 ± 0.1 mM^{-1} s^{-1} was estimated. The reaction with cysteine is complex

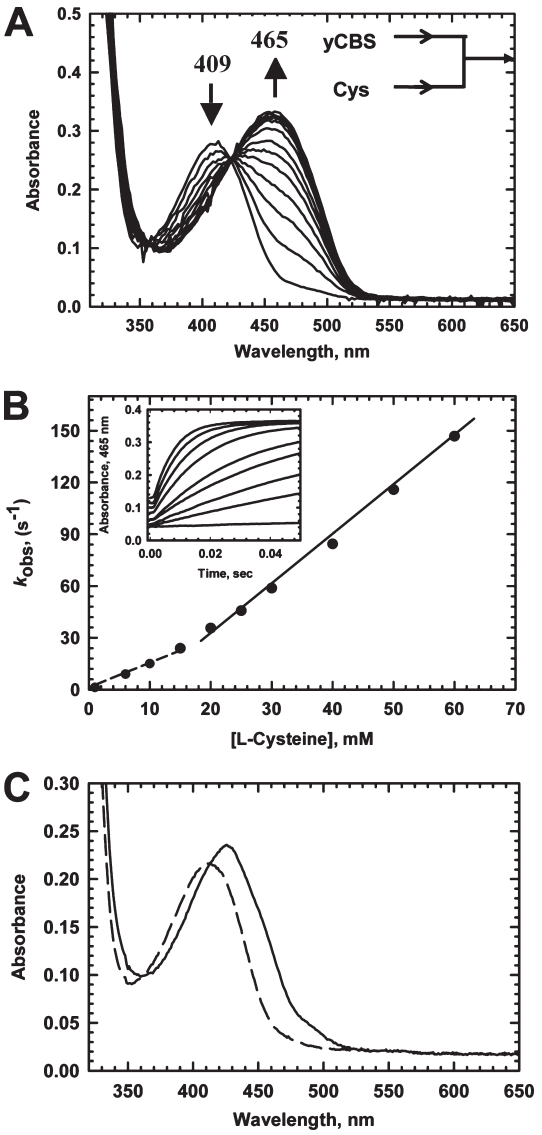

FIGURE 2: Spectra obtained by rapid-scanning stopped-flow spectroscopy of the reaction of yCBS with L-cysteine in 100 mM HEPES buffer (pH 7.4) at 20 °C. (A) yCBS (70 μM) was mixed with 30 mM L-cysteine, and spectra were recorded for 200 ms. The internal aldimine (409 nm), upon addition of L-cysteine, converts to an aminoacrylate species, which has an absorption maximum at 465 nm. This spectral change is observed with isosbestic points at 423 and 357 nm. (B) Dependence of the observed first-order rate constant for the formation of aminoacrylate at 465 nm on the concentration of L-cysteine. The inset shows the kinetics of absorbance changes at 465 nm at various concentrations of cysteine. (C) yCBS (25 μM) was mixed with 10 mM L-cysteine, and spectra were monitored until the 425 nm species was fully formed (—). Addition of 10 mM L-homocysteine led to immediate formation of a 410 nm-absorbing species (– – –).

and includes a mixture of reactions (condensation either with a second mole of cysteine or with a water molecule following β-elimination as shown in reaction 3 or 4, respectively). The maximal rate of reaction 3 is significantly greater than that of reaction 4; however, it is limited by the high K_M of CBS for the second mole of cysteine (33 mM). After reaction for 1−2 s, the absorbance at 465 nm due to the aminoacrylate intermediate decreased, and a new species with an absorbance maximum at 425 nm (Figure 2C) appeared at 0.24 ± 0.02 s^{-1}, which is too slow to be kinetically relevant for cystathionine formation.

Reaction of the Aminoacrylate Intermediate with Homocysteine. Either serine or cysteine can bind to the PLP site and form the aminoacrylate intermediate with the elimination of H_2O or H_2S, respectively. To determine the rate constant for the reaction of the aminoacrylate species with homocysteine, double-mixing experiments were performed. yCBS (120 μM) was mixed with 30 mM serine and aged for 300 ms to preform the aminoacrylate intermediate before the sample was mixed with 0.5−6 mM L-homocysteine (Figure 3A−C). Immediately upon mixing the aminoacrylate with homocysteine, we found an initial decrease in absorbance at 465 nm (Figure 3A); this was followed by steady-state turnover, and when homocysteine was completely consumed because of the presence of excess serine, accumulation of the aminoacrylate, as indicated by the final increase in absorbance at 465 nm, was observed (Figure 3B,C). The duration of the steady-state phase varied with the concentration of homocysteine (Figure 3B) and corresponded well with the expected duration based on the k_{cat} (~8 and ~18 s^{-1} for reactions 1 and 2, respectively) for this reaction. The kinetic course of the reaction in which homocysteine is mixed with the cysteine-derived aminoacrylate is shown in Figure 3D. At the end of the reaction, i.e., when homocysteine is depleted but cysteine is still present, the absorbance at 465 nm decreases because of the formation of the 425 nm-absorbing species as shown in Figure 2C.

The disappearance of the aminoacrylate species was monitored at 465 nm (Figure 3C), and the observed rate constants for this first phase of the reaction were linearly dependent on the concentration of homocysteine (Figure 3B, inset, ○). The bimolecular rate constant was estimated to be 183 ± 4 mM^{-1} s^{-1}, and the apparent k_{off} was 67 ± 4 s^{-1} (y-intercept), yielding a K_d of 0.37 ± 0.02 mM. A plot of the amplitude of the absorbance decrease at 465 nm during the approach to steady state versus the concentration of homocysteine yielded a similar K_{dapp} value of 0.32 ± 0.02 mM.

When homocysteine was added to the aminoacrylate intermediate generated from cysteine (Figure 3B, ●), a comparable value for the bimolecular rate constant was obtained (142 ± 5 mM^{-1} s^{-1}) and the apparent k_{off} was estimated to be 21 s^{-1}. Thus, the K_{dapp} for homocysteine (0.15 ± 0.04 mM), although lower, was similar to the value estimated from the dependence of the change in amplitude at A_{465} during the approach to steady state versus the homocysteine concentration (0.10 ± 0.01 mM).

Reaction of yCBS with Cystathionine. yCBS reacts with cystathionine to form an aminoacrylate species with an absorption maximum at 465 nm (Figure 4). The internal aldimine converts to the aminoacrylate with isosbestic points at 358 and 425 nm, without detectable accumulation of the external aldimine of cystathionine, confirming our previous results (*23*). The rate of aminoacrylate formation, monitored either by the decrease in absorbance at 409 nm or by the increase at 465 nm, was linearly dependent on the concentration of cystathionine. An apparent bimolecular rate constant of 4.1 ± 0.2 mM^{-1} s^{-1} for the formation of the aminoacrylate from cystathionine was obtained from the linear portion of the curve (Figure 4B).

DISCUSSION

The mechanisms by which H_2S elicits its biological effects are poorly understood, but even less is known about how its biosynthesis is enabled or disabled. There is significant pharmacological interest in developing inhibitors of H_2S production as well as H_2S-releasing drugs for treating reperfusion injury, inflammation, and circulatory shock (*26*). Detailed kinetic characterization of the H_2S-generating reactions combined with

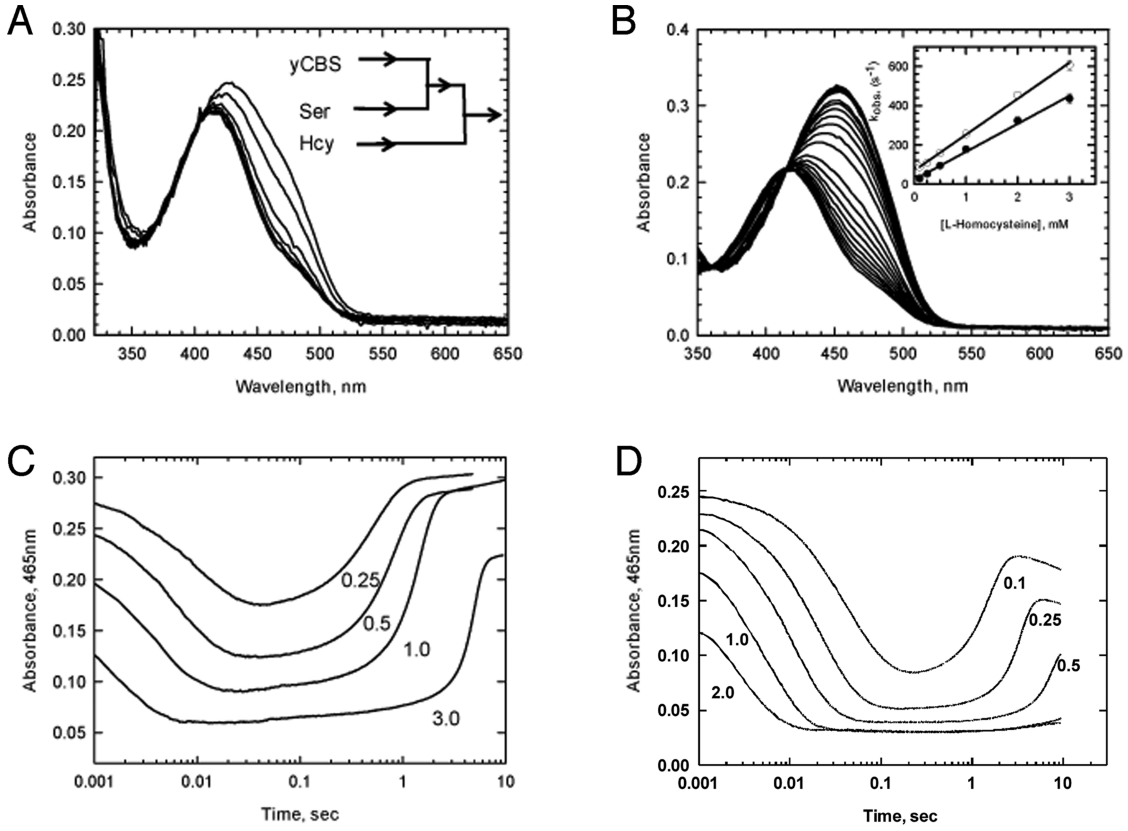

FIGURE 3: Reaction of serine- or cysteine-derived aminoacrylate with homocysteine. (A) yCBS (120 μM) was premixed with 30 mM L-serine to form the aminoacrylate and after 300 ms was mixed with 6 mM L-homocysteine. The spectra are shown for the first 10 ms. (B) Spectral changes for the reaction in panel A monitored for 5 s. This shows the return of the aminoacrylate due to the presence of excess serine. The inset shows the dependence of the observed first-order rate constant for the decrease in absorbance at 465 nm on the concentration of L-homocysteine in the double-mixing experiment. The empty and filled circles represent data from experiments in which yCBS was premixed with serine and cysteine, respectively. (C) Absorbance changes at 465 nm observed with selected homocysteine concentrations (0.25−3 mM after mixing) added to the aminoacrylate derived from serine (as shown in panel A). (D) Reaction of the cysteine-derived aminoacrylate with homocysteine. yCBS (120 μM) was premixed with 12 mM L-cysteine to form the aminoacrylate and, after being aged for 700 ms, was mixed with varying concentrations of L-homocysteine (0.25−2 mM). Absorbance changes at 465 nm are shown.

structural insights into full-length CBS is needed for guiding rational drug design aimed at inhibiting or activating H_2S production by this enzyme. We have recently reported a steady-state characterization of the H_2S-generating reactions catalyzed by the transsulfuration pathway enzymes, CBS and CGL (*11*, *12*). The promiscuous behavior of both enzymes results in a multitude of routes for H_2S production in reactions that depend on the concentrations of the amino acids cysteine and homocysteine. In this study, we present a kinetic characterization of intermediates formed during H_2S biogenesis by yCBS. Because the presence of the heme cofactor in hCBS obscures direct observation of the PLP-bound intermediates, we have employed yCBS, which exhibits robust H_2S producing capacity, as a model for the human enzyme.

The three H_2S-yielding reactions catalyzed by yCBS are described in Scheme 1, and the V/K_{MCys} values for reactions 2−4 are 15.3×10^3, 2.3×10^3, and 0.9×10^3 M^{-1} s^{-1}, respectively. Previously, we reported pre-steady-state kinetic analyses of the canonical yCBS-catalyzed reaction, i.e., the condensation of serine and homocysteine to give cystathionine (*23*). We note that in the earlier work, reactions were studied in 200 mM Tris buffer (pH 8.0) at 15 °C. Amine buffers can form Schiff bases with PLP and therefore are not ideal for studying PLP enzymes. In this study, 100 mM HEPES (pH 7.4) was used, and the temperature was set at 20 °C. These changes resulted in some differences in the kinetic parameters, which are noted below.

When serine is rapidly mixed with yCBS, the internal aldimine converts to the transient species with an apparent second-order rate constant of 38 ± 3 mM^{-1} s^{-1}; this value is ~2.7-fold greater than the value obtained at pH 8.0 and 15 °C (*23*). The maximal rate for formation of the aminoacrylate intermediate was calculated using eq 1 and yielded a value of 155 ± 6 s^{-1}, which is ~10-fold greater than the value reported previously at pH 8 and 15 °C (15 ± 0.4 s^{-1}) (*23*) (Scheme 3A).

When cysteine is rapidly mixed with yCBS, the internal aldimine shows an isosbestic conversion to the aminoacrylate intermediate with apparent second-order rate constants of 1.61 ± 0.04 and 2.8 ± 0.1 mM^{-1} s^{-1}, corresponding to reactions 4 and 3, respectively (Scheme 3B,C). Because an external aldimine did not accumulate at detectable levels in this reaction, we are unable to deconvolute the kinetic parameters for the two steps, i.e., formation of the external aldimine followed by formation of the aminoacrylate. Our data show that the rate of aminoacrylate formation does not depend linearly on the concentration of cysteine (Figure 2). Rather, it appears to be somewhat cooperative. The slope of the curve at lower concentrations of cysteine is ~1.5−2-fold smaller than that at higher concentrations of cysteine. We speculate that binding of the second mole of cysteine (possibly at the site that binds homocysteine in canonical reaction 1) may cause a conformational change or otherwise promote an increase in the rate of aminoacrylate formation. Thus, the biphasic pattern observed during formation of the

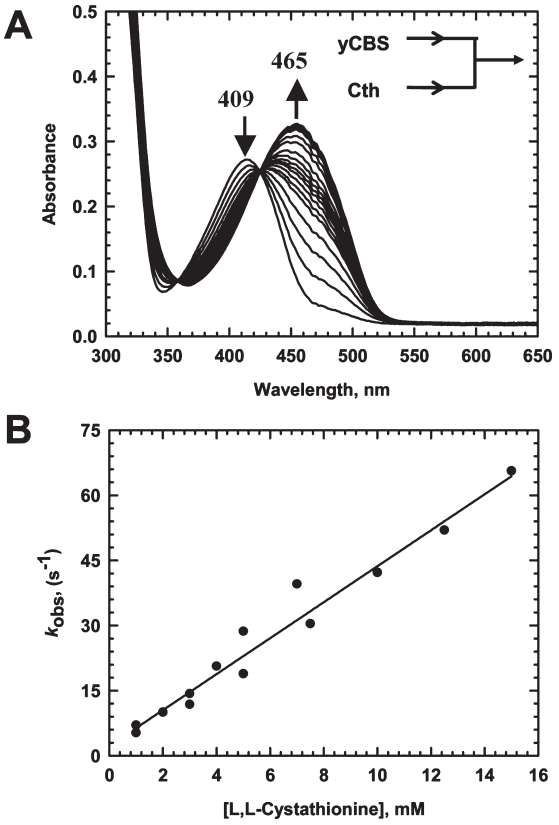

FIGURE 4: Rapid-scanning stopped-flow spectra of the reaction of yCBS with L-cystathionine (Cth) in 100 mM HEPES buffer (pH 7.4) at 20 °C. (A) yCBS (70 μM) was mixed with 20 mM L-cystathionine, and spectra were collected for 100 ms. Upon addition of L-cystathionine, the internal aldimine (409 nm) converts to an aminoacrylate species (465 nm) with isosbestic points at 423 and 357 nm. (B) Plot of the observed first-order rate constant for the formation of the aminoacrylate intermediate on the concentration of L-cystathionine.

aminoacrylate species could correspond to a smaller k_{obs} at low cysteine concentrations when only 1 mol of cysteine is bound at site 1 (the PLP site) and a larger k_{obs} at higher cysteine concentrations when site 2 (occupied by homocysteine in the canonical reaction) is also populated with cysteine. This interpretation is consistent with the steady-state kinetics of H_2S formation, which are clearly biphasic as a function of cysteine concentration (*12*). At low cysteine concentrations, the aminoacrylate intermediate reacts with water to form serine, whereas at high cysteine concentrations, the aminoacrylate intermediate reacts with cysteine bound at site 2.

A few seconds after the reaction with higher concentrations of cysteine (> 6 mM) has proceeded, the aminoacrylate converts to a new species with an absorbance maximum at 425 nm (Figure 2C). The identity of this species is currently not known. However, it is not a dead-end species, because addition of homocysteine to the species with the 425 nm absorbance maximum leads to rapid formation of an aldimine with an absorbance maximum at 409 nm (Figure 2C). From steady-state experiments in which lanthionine formation was monitored, the K_M for cysteine for the second binding site was estimated to be 33 ± 3 mM (*12*). We note that hCBS binds cysteine significantly weaker (K_d = 400 ± 27 μM) than serine (K_d = 56 ± 6 μM) (*12*).

In principle, the aminoacrylate intermediate of yCBS should be the same whether it is formed from serine or cysteine. Hence, the second half-reaction, i.e., the nucleophilic attack of homocysteine on the PLP-bound aminoacrylate species, is also expected to

Scheme 3: Kinetic Mechanism for Reactions Catalyzed by yCBS

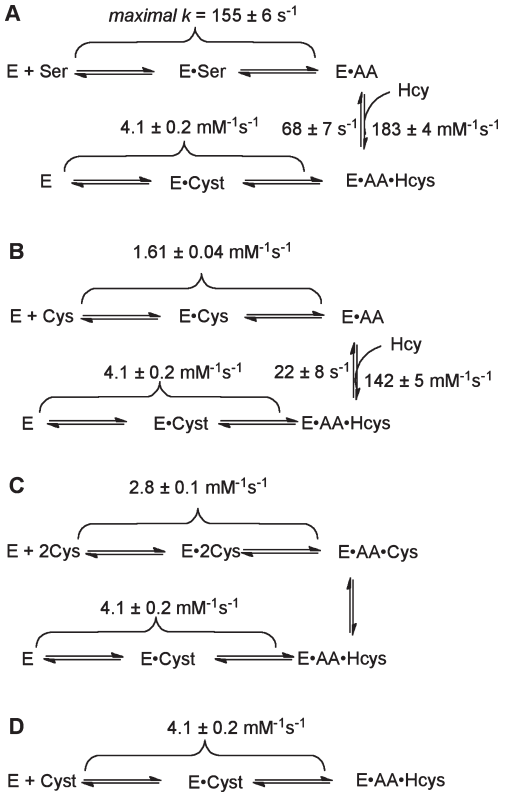

be very similar. Indeed, we found the bimolecular rate constants for the addition of homocysteine to the aminoacrylate intermediate derived from serine or cysteine to be 183 ± 4 and 142 ± 5 mM^{-1} s^{-1}, respectively (Figure 3B, inset). The small difference in these values could be related to the differential release of H_2O versus H_2S in the two reactions that produce the aminoacrylate or to binding of cysteine to a second as yet uncharacterized site. Surprisingly, the k_{off} observed in the case of serine with homocysteine is ~3-fold larger than for cysteine with homocysteine (*y*-intercepts in Figure 3B, inset). The basis for this difference is presently not understood. In the case of the reaction involving serine with homocysteine, the K_d for homocysteine was determined to be 0.37 ± 0.02 mM, whereas for the reaction involving cysteine with homocysteine, the K_d for homocysteine was determined to be 0.15 ± 0.03 mM. This value is similar to the K_M (0.13 ± 0.02 mM) for homocysteine determined for the reaction involving cysteine with homocysteine.

The bimolecular rate constant for the reaction of cystathionine with yCBS to form the aminoacrylate (4.1 ± 0.2 mM^{-1} s^{-1} at 20 °C) is ~3-fold larger than the value determined previously using Tris buffer at pH 8.0 and 15 °C (1.5 mM^{-1} s^{-1}), and the K_{dapp} for cystathionine is ~3-fold smaller than that previously determined (1.6 ± 0.3 mM) (*18*) (Scheme 3D). However, because we are unable to detect an external aldimine, the k_{obs} represents a composite of the binding and chemical steps. We note that the k_{cat} values for reactions 1 (serine with homocysteine) and 2 (cysteine with homocysteine) are ~8 and ~18 s^{-1}, respectively, at 20 °C, which match well the estimates obtained from the duration of the steady-state phase in the rapid reaction kinetic data (Figures 3C,D). Because cystathionine is a common product in these two reactions, its release rate could not be completely rate determining, because it would not account for the difference in the k_{cat} values for the two reactions. Furthermore, differences in

the leaving group potential of water from serine versus the H_2S from cysteine are also unlikely to account for the ~2-fold difference in the k_{cat} between reactions 1 and 2, because formation of the aminoacrylate from serine is rapid (155 s^{-1}), i.e., ~20-fold higher than k_{cat}. Instead, under steady-state turnover conditions, differences in the rate of release of water (reaction 1) versus H_2S (reaction 2) and/or a kinetically invisible conformational change is likely to contribute to the ~2-fold difference in the turnover numbers for these reactions.

ACKNOWLEDGMENT

We acknowledge Dr. Dominique Padovani for help with the initial set up of the experiments and Dr. Tatyana Spolitak for help with Specfit analysis and an anonymous reviewer of the manuscript for helpful discussions on our treatment of the kinetic data, particularly in Figure 1.

REFERENCES

1. Wang, R. (2002) Two's company, three's a crowd: Can H2S be the third endogenous gaseous transmitter? *FASEB J. 16*, 1792–1798.
2. Kimura, H. (2002) Hydrogen sulfide as a neuromodulator. *Mol. Neurobiol. 26*, 13–19.
3. Kabil, O., and Banerjee, R. (2010) The redox biochemistry of hydrogen sulfide. *J. Biol. Chem. 285*, 21903–21907.
4. Yang, G., Wu, L., Jiang, B., Yang, W., Qi, J., Cao, K., Meng, Q., Mustafa, A. K., Mu, W., Zhang, S., Snyder, S. H., and Wang, R. (2008) H2S as a physiologic vasorelaxant: Hypertension in mice with deletion of cystathionine γ-lyase. *Science 322*, 587–590.
5. Elrod, J. W., Calvert, J. W., Morrison, J., Doeller, J. E., Kraus, D. W., Tao, L., Jiao, X., Scalia, R., Kiss, L., Szabo, C., Kimura, H., Chow, C. W., and Lefer, D. J. (2007) Hydrogen sulfide attenuates myocardial ischemia-reperfusion injury by preservation of mitochondrial function. *Proc. Natl. Acad. Sci. U.S.A. 104*, 15560–15565.
6. Sivarajah, A., Collino, M., Yasin, M., Benetti, E., Gallicchio, M., Mazzon, E., Cuzzocrea, S., Fantozzi, R., and Thiemermann, C. (2009) Anti-apoptotic and anti-inflammatory effects of hydrogen sulfide in a rat model of regional myocardial I/R. *Shock 31*, 267–274.
7. Sohn, H., and Kuriyama, H. (2001) Ultradian metabolic oscillation of *Saccharomyces cerevisiae* during aerobic continuous culture: Hydrogen sulphide, a population synchronizer, is produced by sulphite reductase. *Yeast 18*, 125–135.
8. Stipanuk, M. H., and Beck, P. W. (1982) Characterization of the enzymic capacity for cysteine desulphhydration in liver and kidney of the rat. *Biochem. J. 206*, 267–277.
9. Shibuya, N., Tanaka, M., Yoshida, M., Ogasawara, Y., Togawa, T., Ishii, K., and Kimura, H. (2009) 3-Mercaptopyruvate sulfurtransferase produces hydrogen sulfide and bound sulfane sulfur in the brain. *Antioxid. Redox Signaling 11*, 703–714.
10. Ishii, I., Akahoshi, N., Yamada, H., Nakano, S., Izumi, T., and Suematsu, M. (2010) Cystathionine γ-lyase-deficient mice require dietary cysteine to protect against acute lethal myopathy and oxidative injury. *J. Biol. Chem. 285*, 26358–26368.
11. Chiku, T., Padovani, D., Zhu, W., Singh, S., Vitvitsky, V., and Banerjee, R. (2009) H2S biogenesis by cystathionine γ-lyase leads to the novel sulfur metabolites, lanthionine and homolanthionine, and is responsive to the grade of hyperhomocysteinemia. *J. Biol. Chem. 284*, 11601–11612.
12. Singh, S., Padovani, D., Leslie, R. A., Chiku, T., and Banerjee, R. (2009) Relative contributions of cystathionine β-synthase and γ-cystathionase to H2S biogenesis via alternative trans-sulfuration reactions. *J. Biol. Chem. 284*, 22457–22466.
13. Koutmos, M., Kabil, O., Smith, J. L., and Banerjee, R. (2010) Structural basis for substrate activation and regulation by cystathionine β-synthase (CBS) domains in cystathionine β-synthase. *Proc. Natl. Acad. Sci. U.S.A. 107*, 20958–20963.
14. Banerjee, R., Evande, R., Kabil, O., Ojha, S., and Taoka, S. (2003) Reaction mechanism and regulation of cystathionine β-synthase. *Biochim. Biophys. Acta 1647*, 30–35.
15. Miles, E. W., and Kraus, J. P. (2004) Cystathionine β-Synthase: Structure, Function, Regulation, and Location of Homocystinuria-causing Mutations. *J. Biol. Chem. 279*, 29871–29874.
16. Mudd, S. H., Levy, H. L., and Kraus, J. P. (2001) Disorders of Transsulfuration. In The Online Metabolic and Molecular Bases of Inherited Disease (Scriver, C. R., Beaudet, A. L., Sly, W. S., Valle, D., Vogelstein, B., Kinzler, K. W., and Childs, B., Eds.) pp 2007−2056, McGraw-Hill, New York.
17. Meier, M., Janosik, M., Kery, V., Kraus, J. P., and Burkhard, P. (2001) Structure of human cystathionine β-synthase: A unique pyridoxal 5′-phosphate-dependent heme protein. *EMBO J. 20*, 3910–3916.
18. Eliot, A. C., and Kirsch, J. F. (2004) Pyridoxal phosphate enzymes: Mechanistic, structural, and evolutionary considerations. *Annu. Rev. Biochem. 73*, 383–415.
19. Drewe, W. F., Jr., and Dunn, M. F. (1985) Detection and identification of intermediates in the reaction of L-serine with *Escherichia coli* tryptophan synthase via rapid-scanning ultraviolet-visible spectroscopy. *Biochemistry 24*, 3977–3987.
20. Woehl, E. U., Tai, C. H., Dunn, M. F., and Cook, P. F. (1996) Formation of the α-aminoacrylate immediate limits the overall reaction catalyzed by O-acetylserine sulfhydrylase. *Biochemistry 35*, 4776–4783.
21. Taoka, S., West, M., and Banerjee, R. (1999) Characterization of the heme and pyridoxal phosphate cofactors of human cystathionine β-synthase reveals nonequivalent active sites. *Biochemistry 38*, 2738–2744.
22. Evande, R., Ojha, S., and Banerjee, R. (2004) Visualization of PLP-bound intermediates in hemeless variants of human cystathionine β-synthase: Evidence that lysine 119 is a general base. *Arch. Biochem. Biophys. 427*, 188–196.
23. Taoka, S., and Banerjee, R. (2002) Stopped-flow kinetic analysis of the reaction catalyzed by the full-length yeast cystathionine β-synthase. *J. Biol. Chem. 277*, 22421–22425.
24. Jhee, K. H., Niks, D., McPhie, P., Dunn, M. F., and Miles, E. W. (2001) The reaction of yeast cystathionine β-synthase is rate-limited by the conversion of aminoacrylate to cystathionine. *Biochemistry 40*, 10873–10880.
25. Jhee, K. H., McPhie, P., and Miles, E. W. (2000) Yeast cystathionine β-synthase is a pyridoxal phosphate enzyme but, unlike the human enzyme, is not a heme protein. *J. Biol. Chem. 275*, 11541–11544.
26. Szabo, C. (2007) Hydrogen sulphide and its therapeutic potential. *Nat. Rev. Drug Discovery 6*, 917–935.